





Prognostic prediction of resectable colorectal liver metastasis using the apparent diffusion coefficient from diffusion-weighted magnetic resonance imaging

Masato Yoshikawa  | Yuji Morine  | Shinichiro Yamada  | Katsuki Miyazaki |
 Kazunori Tokuda  | Yu Saito  | Yusuke Arakawa | Tetsuya Ikemoto  |
 Satoru Imura  | Mitsuo Shimada

Department of Surgery, Institute of Biomedical Sciences, University of Tokushima, Tokushima, Japan

Correspondence

Yuji Morine, Department of Surgery, Institute of Biomedical Sciences, University of Tokushima, 3-18-15 Kuramoto-cho, Tokushima City, 770-8503, Japan.
 Email: ymorine@tokushima-u.ac.jp

Abstract

Aim: Diffusion-weighted magnetic resonance imaging (DWI-MRI) is used to predict tumor malignancy. Here we explored the role of apparent diffusion coefficient (ADC) values in the treatment of patients with resectable colorectal liver metastasis (CRLM).

Methods: Magnetic resonance imaging (MRI) scans were conducted using a Signa HD or Signa Explorer 1.5-T scanner (GE Healthcare). ADC maps were calculated using DWI with b values of 0, 20, and 800 s/mm². We enrolled 60 patients who underwent upfront hepatic resection for CRLM and divided them into ADC-high ($n = 30$) and ADC-low ($n = 30$) groups. Clinicopathological variables of the groups were compared. Immunohistochemical analysis of HIF-1 α expression in tumor tissues was performed, and the relationship between the ADC value and HIF-1 α expression was evaluated.

Results: The disease-free survival rate of the ADC-low group was significantly lower than that of the ADC-high group ($P < .05$). Univariate analysis revealed that tumor number (more than five), synchronous metastasis, and low ADC were prognostic factors. Multivariate analysis identified low ADC as an independent prognostic factor. Furthermore, the ADC-low group more frequently expressed high levels of HIF-1 α than the ADC-high group.

Conclusion: Low ADC values were an independent prognostic factor of resectable CRLM and correlated with HIF-1 α expression.

KEYWORDS

apparent diffusion coefficient, colorectal liver metastasis, hypoxia inducible factor-1, magnetic resonance imaging, prognostic prediction

1 | INTRODUCTION

Colorectal liver metastasis (CRLM) is the most frequent type of metastasis, occurring in 15%-25% of patients with colorectal cancer at first diagnosis,^{1,2} and in as much as 50% of patients during the first

3 years after resection of the primary cancer.³⁻⁵ The only potential curative treatment for CRLM is surgical resection,⁶ which is recommended as upfront surgery for technically easy CRLM, according to the European Society for Medical Oncology (ESMO) consensus guidelines.^{7,8}

This is an open access article under the terms of the Creative Commons Attribution-NonCommercial-NoDerivs License, which permits use and distribution in any medium, provided the original work is properly cited, the use is non-commercial and no modifications or adaptations are made.

© 2020 The Authors. Annals of Gastroenterological Surgery published by John Wiley & Sons Australia, Ltd on behalf of The Japanese Society of Gastroenterology

Diffusion-weighted magnetic resonance imaging (DWI-MRI), which can be added to routine MRI without requiring a contrast agent, may provide information regarding tissue and tumor microstructures.⁹⁻¹¹ The apparent diffusion coefficient (ADC) derived from DWI can be used to quantitate the diffusivity of water. ADC values are influenced by factors such as fibrosis, cellularity, cell membrane integrity, extracellular fibrosis, and glandular formations. ADC values have clinical utility for characterizing tumor tissues,¹²⁻¹⁹ staging tumors,¹⁶⁻¹⁸ and predicting treatment outcomes.²⁰⁻²² For example, low ADC values are an independent prognostic factor for survival of patients with pancreatic cancer,²³ and the ADC values of those with breast cancer negatively correlate with tumor stromal density.²⁴ CRLM exhibits characteristically high stromal density.

Stromal desmoplasia leads to decreased blood supply, poor drug delivery, and hypoxia.^{25,26} Although hypoxia presents a particularly hostile environment for cell growth, cancer cells adapt and survive by increasing the expression of genes responsible for anaerobic metabolism, cell survival, metastasis, and angiogenesis.²⁷ The cellular response to hypoxia is mediated through a rapid increase in the level of the transcription factor hypoxia inducible factor-1 α (HIF-1 α).²⁸ For example, increased HIF-1 α activity mediates the induction of desmoplasia of pancreatic cancer, which is amplified by cycles of decreased blood flow, increased hypoxia, and tumor malignancy.²⁸ Therefore, we investigated the utility of ADC values in association with HIF-1 α expression levels for predicting the prognosis of patients with CRLM.

2 | METHODS

2.1 | Patients

We enrolled 60 patients with CRLM who underwent radical resection at Tokushima University Hospital between April 2005 and June 2017. These patients underwent upfront liver radical resection as initial treatment of CRLM, and radical resections were confirmed with pathological examinations. Diagnosis and classification of the tumors were determined according to the International Union Against Cancer (UICC 8th edition) staging system. Other eligibility criteria included no neoadjuvant chemotherapy, available MRI examinations including DWI obtained within 4 weeks before resection, and a hepatic mass >1 cm (as indicated by anatomical MRI) to allow accurate

ADC measurements. One patient was excluded by the hepatic mass <1 cm. Follow-up ranged from 1.14-9.72 years (median, 3.39 years). Our hospital's ethics committee approved this retrospective study, and written informed consent for the use of their resected tissues was obtained from all patients (approval no. 3341). The study conformed to the provisions of the Declaration of Helsinki (as revised in Fortaleza, Brazil, October 2013), available at: <http://www.wma.net/en/30publications/10policies/b3/>.

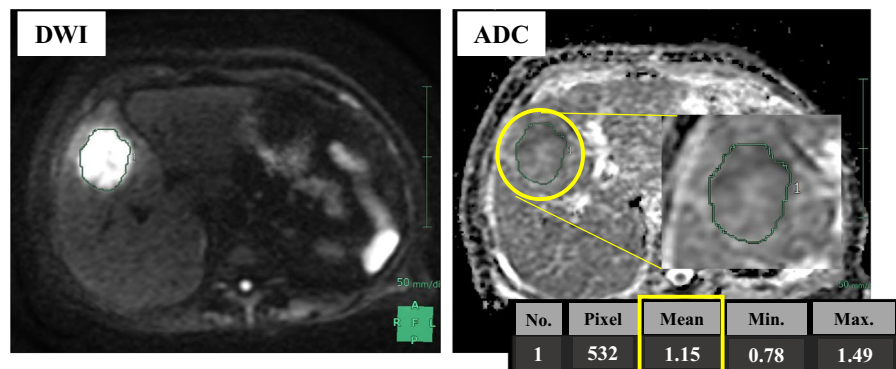
2.2 | Magnetic resonance imaging protocol

Magnetic resonance imaging scans were conducted using a Signa HDe or Signa Explorer 1.5-T scanner (GE Healthcare) with an eight-channel phased-array coil. Fast spin-echo T2-weighted images (T2W) and DWI ($b = 0, 20, 800$ s/mm²) were obtained. The mean ADC values ($\times 10^{-3}$ mm²/s) of tumors were measured in regions of interest (ROI) with manual tracing from ADC maps using Synapse Vincent software (FujiFilm Medical), which automatically calculates the mean, minimum, and maximum values that are displayed as a free-form green line (Figure 1). The mean ADC value chosen was consistent with the literature. ROIs included most of the areas of the homogeneous solid portions of tumors while avoiding the most peripheral portions to exclude partial-volume effects of adjacent uninvolved tissues.²⁹ In multiple metastasis cases, we measured its greatest diameter in the axial plane on non-contrast T1W images. When the tumor had a necrotic component, conventional T2W, DWI, and contrast-enhanced T1W images were used, avoiding cystic or necrotic parts.³⁰ We used the median ADC value (1.27×10^{-3} mm²/s) as the cut-off to divide patients into ADC-high ($n = 30$) and ADC-low ($n = 30$) groups.

2.3 | Patient follow-up

We followed subjects as outpatients according to a standard protocol.³¹ Briefly, follow-up was performed every 2 months during the first year after surgery and at least every 3-4 months thereafter. Carcinoembryonic antigen (CEA) was evaluated at each assessment. Abdominal dynamic computed tomography (CT) was performed every 6 months. Recurrence was diagnosed according to its characteristic appearance on CT, MRI, or both.^{32,33} Intrahepatic

FIGURE 1 Analysis of the apparent diffusion constant (ADC). ADC values were obtained by manually drawing a region of interest (ROI) within the largest area of the tumor on each ADC map. DWI, diffusion-weighted MRI



recurrence of CRLM was diagnosed when certain criteria were met, as follows: the lesion was enhanced during the arterial phase; the lesion was enhanced, hypoattenuated, or hypointense compared with the surrounding liver during the venous or delayed phases, or both. Additional imaging findings regarded as suggestive but not diagnostic of intrahepatic recurrence of CRLM were as follows: lesion exhibiting arterial ring enhancement or delayed enhancement compared with the surrounding liver during the venous or delayed phases, or both; peripheral rim enhancement during the delayed phase; decreased signal intensity during the liver-specific hepatobiliary phase; and moderately increased signal intensity on T2-weighted MRI. An elevated level of CEA was considered when determining recurrence.

2.4 | Immunohistochemical analysis of HIF-1 α expression

Archived formalin-fixed paraffin-embedded tissue blocks were cut into 4- μ m-thick sections. The samples were deparaffinized and dehydrated using a graded series of ethanol concentrations. Endogenous peroxidase activity was inhibited using 0.3% hydrogen peroxidase and methanol for 20 minutes. After rinsing in phosphate-buffered saline (PBS), the tissue sections were processed in 0.01 mol/L citrate buffer (pH 6.0) in a heat-resistant plastic container. The sections were then irradiated in a consumer-grade microwave oven for 20 minutes, and the slides were allowed to cool at room temperature. The sections were incubated overnight at 4°C with a mouse monoclonal antibody against HIF-1 α (diluted 1:500) (H1 α 67, NB100-105; Novus Biologicals). After rinsing overnight, the sections were incubated with Dako REAL EnVision Detection System, Peroxidase/DAB+, Rabbit/Mouse for 45 minutes, followed by three washes in PBS, after which immune complexes were visualized using 3,3'-diaminobenzidine tetrahydrochloride for 5 minutes. Nuclei were counterstained using Mayer's hematoxylin solution.

Cells counts were performed using a microscope equipped with a Nikon DXM 1200F camera at a magnification of $\times 200$ ($\times 20$ objectives and $\times 10$ eyepieces). The regions counted in each section were randomly selected from a representative field of the tumor. Eight regions were assessed for each section, and the counts are expressed as the mean percentage of positive tumor cells in high-power fields.³⁴ Immunostaining was evaluated by a pathologist who was uninformed of patients' clinical characteristics. HIF-1 α expression was evaluated according to scoring intensity (0, negative; 1, low; 2, medium; 3, high) as well as the extent of staining (0, 0%; 1, 1%–25%; 2, 26%–50%; 3, $\geq 51\%$). The score was defined as intensity (0–3) plus area (0–3), low 0–3, and high ≥ 4 .

2.5 | Statistical analysis

Statistical analyses were performed using JMP 10.0.2 software (SAS Campus Drive). All results are expressed as the mean \pm standard error. The Mann-Whitney test was used to compare continuous

variables, and the chi-square test was used for categorical data. Survival rates were calculated using the Kaplan-Meier product-limit method. Differences in survival between groups were compared using the log rank test. Prognostic factors were evaluated using univariate and multivariate analyses (Cox proportional hazards regression model). Continuous variables were generally classified into two groups according to the median value of each variable, and $P < .05$ indicates a significant difference.

3 | RESULTS

3.1 | Patients' clinicopathological characteristics

All patients with resectable CRLM underwent primary radical hepatectomy, and data other than the histopathological findings were acquired immediately before surgery. Histopathological diagnosis was determined after surgery. Table 1 shows that the clinicopathological

TABLE 1 Associations between clinicopathological factors and ADC values

Factors	ADC high (n = 30)	ADC low (n = 30)	P value
Age (y) (≤ 65 / > 65)	10/20	10/20	1.00
Sex (male/ female)	22/8	17/13	.17
Primary site			
Location (colon/ rectum)	17/13	19/11	.60
Differentiation (Tub1/ Others)	10/20	3/27	.08
Lymphatic invasion (\pm)	16/14	13/17	.36
Vessel invasion (\pm)	5/25	6/24	.32
Metastatic site			
Metastatic period (synchro/ metachro)	12/18	18/12	.12
Tumor number (≤ 4 / > 5)	26/4	24/6	.49
Maximum diameter (≤ 5 cm/ > 5 cm)	27/3	26/4	.69
CEA (≤ 5 ng/mL/ > 5 ng/mL)	10/20	12/18	.47
CA19-9 (≤ 37 U/mL/ > 37 U/mL)	21/9	21/9	1.00
Adjuvant chemotherapy (\pm)			
UFT/ LV	4 (30.7)	5 (41.7)	
mFOLFOX6	1 (7.7)	2 (16.7)	
IRIS	0 (0)	1 (8.3)	
XELOX	3 (23.1)	2 (16.7)	
XELODA	2 (15.4)	1 (8.3)	
SOX	0 (0)	1 (8.3)	
S-1	3 (23.1)	0 (0)	

Abbreviations: CA19-9, carbohydrate antigen 19-9; CEA, carcinoembryonic antigen; metastasis metachro, metachronous metastasis; synchro, synchronous; Tub1: well-differentiated tubular adenocarcinoma.

variables of patients in the ADC-low and the ADC-high groups were not significantly different. Specifically, the groups did not significantly differ in sex, age, and tumor factors such as tumor size, location, differentiation, lymphatic invasion, vessel invasion, metastatic period, tumor number, maximum diameter, and tumor markers. The rates of adjuvant chemotherapy were not significantly different between two groups.

3.2 | Apparent diffusion coefficient values and overall and disease-free survival rates

There was no significant difference in overall survival between the ADC-high and ADC-low groups (5-year survival rates: ADC-high group, 68.7%; ADC-low group, 50.0%; $P = .71$). However, the ADC-low group experienced significantly shorter disease-free survival than the ADC-high group (5-year disease-free survival rates: ADC-high group, 52.8%; ADC-low group, 26.3%; $P = .02$; Figure 2). Univariable analysis of risk factors for tumor recurrence revealed that multiple tumors (more than five), synchronous metastasis, and low ADC values were significant risk factors for tumor recurrence. Multivariate analysis identified low ADC (hazard ratio, 2.01; 95% CI, 1.01-4.16) as an independent predictive factor for recurrence (Table 2).

3.3 | Correlation between ADC values and HIF-1 α expression

We investigated the correlation between the ADC value and HIF-1 α expression in tumor tissue. Representative stainings of HIF-1 α of tumor tissue are shown in Figure 3A. HIF-1 α staining scores was significantly higher in the ADC-low group than in the ADC-high group ($P = .03$; Figure 3B). A representative case is shown in Figure 4, in which HIF-1 α expression was significantly increased in the low ADC ROI.

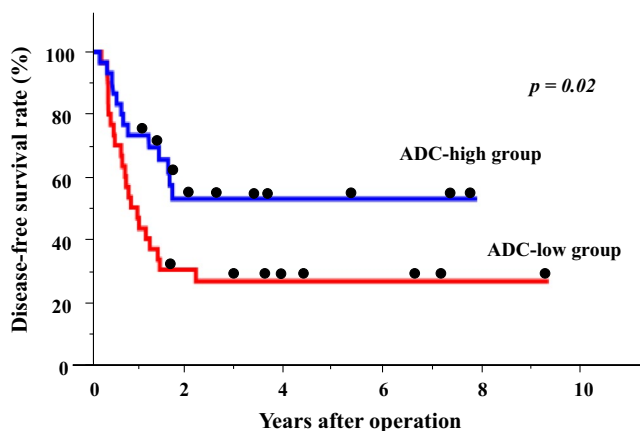


FIGURE 2 Kaplan-Meier analysis of disease-free survival rates. Blue = ADC-high group (n = 30), red = ADC-low group (n = 30)

4 | DISCUSSION

Here we evaluated the associations among preoperative ADC values, prognosis after surgery, and clinicopathological parameters of CRLM. We found significant associations between ADC and HIF-1 α expression as well as between the recurrence-free survival rate after surgery. Moreover, we found significant negative correlations between ADC and HIF-1 α expression. Our results suggest that ADC values are closely associated with tumor proliferation and hypoxia and therefore may serve as an imaging biomarker for CRLM.

Most tumor markers used for clinical management, diagnosis, grading, progression, aggressiveness, and prognosis are measured using immunohistochemistry, which requires invasive tissue sampling.³⁵ Noninvasive methods to assess tumor characteristics are therefore required. The noninvasive DWI-MRI method evaluated here provides information on the microscopic structure of tissue by measuring the diffusion of water molecules within a tissue.^{36,37}

The ADC derived from DWI is used as an imaging biomarker to predict histopathologic grade, therapeutic response, and prognosis of certain tumors, including CRLM.³⁸⁻⁴² For example, Ki-67 expression is significantly related to the Gleason score (GS) of prostate cancer and can be applied together with GS as a prognostic factor. Ki-67 expression positively correlates with GS and inversely with ADC. Moreover, there is a significant difference between low and high expression of Ki-67 associated with higher Ki-67 expression and lower ADC values.⁴³ Furthermore, there is a negative correlation between ADC values and expression of Ki-67 for other cancers.¹⁷

In certain solid tumors, hypoxia and correspondingly high levels of HIF-1 α activity influence tumor invasiveness, metastasis, and resistance to radiotherapy and chemotherapy.²⁷ Similarly, high HIF-1 α expression is associated with metastasis, resistance to radiotherapy, chemoresistance, and biochemical recurrence in patients with CRLM.⁴⁴ Unfortunately, noninvasive clinical methods to assess the expression of HIF-1 α in CRLM are unavailable.

Here we found a negative correlation between HIF-1 α expression and ADC in CRLM. To the best of our knowledge, this is the first report of an association between the ADC and HIF-1 α expression in CRLM. Hypoxia may inhibit the growth of tumor cells or cause their death through the induction of biochemical changes required for cells to adapt to an environment in which the diffusion of water may decrease.⁴⁵ We conclude, therefore, that under hypoxic conditions, high HIF-1 α expression is associated with a reduction in ADC values.

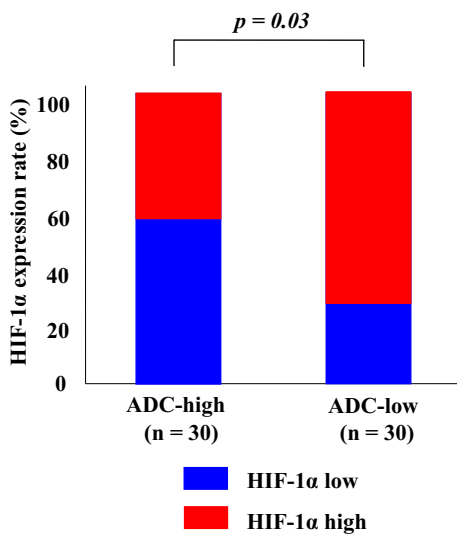
Angiogenesis, which is required for the growth of a primary tumor and the development of metastasis, affects the growth, invasiveness, and metastasis of colorectal cancer cells. Vascular endothelial growth factor (VEGF) is required for angiogenesis. Under hypoxic conditions, HIF-1 α activates the expression of many downstream genes, including VEGF. Moreover, expression of the genes encoding HIF-1 α and VEGF is upregulated in CRLM.⁴³

Several limitations must be considered when interpreting the results of our study. First, the patient population was relatively small, further study with a larger population might be necessary

Factors	Univariate analysis		Multivariate analysis	
	5-year DFS (%)	P value	HR (95%CI)	P value
Primary site				
Location (colon/ rectum)	40.1 vs 32.3	.84		
Differentiation (Tub1/ others)	44.0 vs 33.8	.47		
Lymphatic invasion (-/+)	43.7 vs 36.6	.42		
Vessel invasion (-/+)	42.9 vs 22.2	.38		
Metastatic site				
Metastatic period (metachro/ synchro)	45.1 vs 28.8	.03	1.60 (0.81-3.23)	.17
Number (≤ 4 / > 5)	43.1 vs 27.4	.04	1.68 (0.67-3.69)	.24
Maximum diameter (≤ 5 cm/ > 5 cm)	32.6 vs 52.6	.30		
CEA (< 5 ng/mL/ > 5 ng/mL)	51.6 vs 34.6	.35		
CA19-9 (< 37 U/mL/ > 37 U/mL)	39.9 vs 37.5	.68		
Adjuvant chemotherapy (-/+)	32.7 vs 41.7	.93		
ADC (high/ low)	52.8 vs 26.3	.02	2.03 (1.02-4.19)	.04

Abbreviations: ADC, apparent diffusion coefficient; CA19-9, carbohydrate antigen 19-9; CEA, carcinoembryonic antigen; metachro, metachronous metastasis; synchro, synchronous metastasis; Tub1, well-differentiated tubular adenocarcinoma.

(A)



(B)

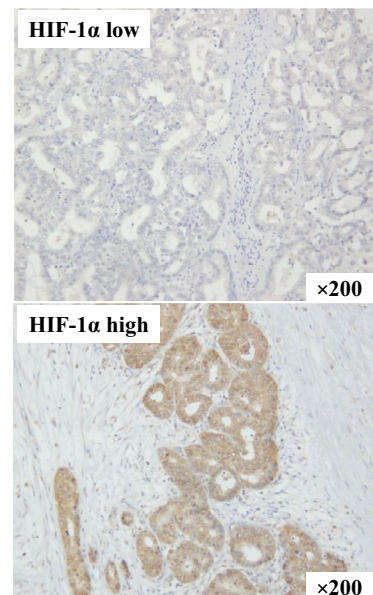
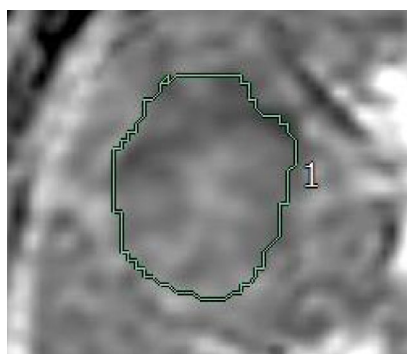
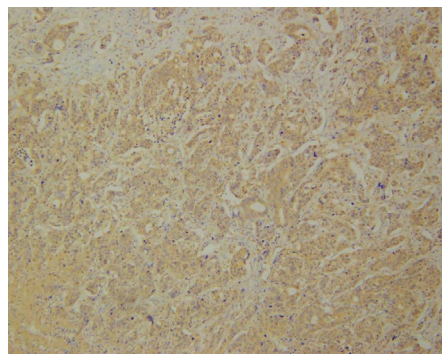


TABLE 2 Predictive factors of disease-free survival

FIGURE 3 Correlation between ADC values and HIF-1 α expression in tumor tissues. (A) Representative immunohistochemical detection of HIF-1 α . (B) Blue = low HIF-1 α expression, red = high HIF-1 α expression



ADC low



HIF-1 α high

FIGURE 4 A representative case showing the correlation between low ADC and high HIF-1 α expression

to strengthen our result. Second, we did not determine the reproducibility of the ADC values. Third, selection bias was possible because of the retrospective nature of our study, which analyzed only patients with CRLM who underwent MRI. In addition, our result showed that there was no significant difference in overall survival rate between the ADC-high and ADC-low groups. The reason why overall survival rate was not different in CRLM was that the difference of the treatment rate after recurrence, such as re-hepatectomy, variety of chemotherapy, was higher than other cancers, especially pancreatic cancer.²³ Furthermore, we followed up strictly and detected the recurrence at an early stage for early therapeutic intervention, such as re-hepatectomy.

Our present studies provide compelling evidence to support the conclusion that the ADC value reflects tumorigenesis under hypoxic conditions through the expression of HIF-1 α . The ADC value may therefore serve as a surrogate marker of tumor malignancy.

5 | CONCLUSION

Low ADC values serve as an independent prognostic factor and correlate with HIF-1 α expression in CRLM. The ADC value can be used as a surrogate marker for recurrence of CRLM.

ACKNOWLEDGEMENTS

Yuji Morine, Shinichiro Yamada, Katsuki Miyazaki, Kazunori Tokuda, Yu Saito, Yusuke Arakawa, Tetsuya Ikemoto, Satoru Imura, and Mitsuo Shimada declare that no competing interests exist. We thank Edanz Group (www.edanzediting.com/ac) for editing a draft of this manuscript.

DISCLOSURE

Conflicts of interests: Authors declare no conflicts of interest for this article.

ORCID

Masato Yoshikawa  <https://orcid.org/0000-0002-0621-0602>

Yuji Morine  <https://orcid.org/0000-0002-5889-9288>

Shinichiro Yamada  <https://orcid.org/0000-0003-3847-751X>

Kazunori Tokuda  <https://orcid.org/0000-0003-4036-6325>

Yu Saito  <https://orcid.org/0000-0001-6349-1669>

Tetsuya Ikemoto  <https://orcid.org/0000-0001-9800-1359>

Satoru Imura  <https://orcid.org/0000-0003-0368-990X>

REFERENCES

- Fong Y, Kemeny N, Paty P, Blumgart LH, Cohen AM. Treatment of colorectal cancer: hepatic metastasis. *Semin Surg Oncol.* 1996;12:219–52.
- Ruers T, Bleichrodt RP. Treatment of liver metastases, an update on the possibilities and results. *Eur J Cancer.* 2002;38:1023–33.
- Steele GJ, Ravikumar TS. Resection of hepatic metastases from colorectal carcinoma: biologic perspectives. *Ann Surg.* 1989;210:127–38.
- O'Reilly DA, Poston GJ. Colorectal liver metastases: current and future perspectives. *Future Oncol.* 2006;2:525–31.
- Haruki K, Shiba H, Fujiwara Y, Furukawa K, Wakiyama S, Ogawa M, et al. Perioperative change in peripheral blood monocyte count may predict prognosis in patients with colorectal liver metastasis after hepatic resection. *J Surg Oncol.* 2012;106:31–5.
- Watanabe T, Muro K, Ajioka Y, Hashiguchi Y, Ito Y, Saito Y, et al. Japanese Society for Cancer of the Colon and Rectum: Japanese Society for Cancer of the Colon and Rectum (JSCCR) guidelines 2016 for the treatment of colorectal cancer. *Int J Clin Oncol.* 2018;23:1–34.
- Van Cutsem E, Cervantes A, Adam R, Sobrero A, Van Krieken JH, Aderka D, et al. ESMO consensus guidelines for the management of patients with metastatic colorectal cancer. *Ann Oncol.* 2016;27:1386–422.
- Yoshino T, Arnold D, Taniguchi H, Pentheroudakis G, Yamazaki K, Xu RH, et al. Pan-Asian adapted ESMO consensus guidelines for the management of patients with metastatic colorectal cancer: a JSMO–ESMO initiative endorsed by CSCO, KACO, MOS, SSO and TOS. *Ann Oncol.* 2018;29:44–70.
- Lang P, Wendland MF, Saeed M, Gindele A, Rosenau W, Mathur A, et al. Osteogenic sarcoma: noninvasive in vivo assessment of tumor necrosis with diffusion-weighted MR imaging. *Radiology.* 1998;206:227–35.
- Sandrasegaran K, Akisik FM, Lin C, Tahir B, Rajan J, Saxena R, et al. Value of diffusion-weighted MRI for assessing liver fibrosis and cirrhosis. *AJR Am J Roentgenol.* 2009;193:1556–60.
- Padhani AR, Liu G, Koh DM, Chenevert TL, Thoeny HC, Takahara T, et al. Diffusion-weighted magnetic resonance imaging as a cancer biomarker: consensus and recommendations. *Neoplasia.* 2010;11:102–25.
- Yoshikawa MI, Ohsumi S, Sugata S, Kataoka M, Takashima S, Mochizuki T, et al. Relation between cancer cellularity and apparent diffusion coefficient values using diffusionweighted magnetic resonance imaging in breast cancer. *Radiat Med.* 2008;26:222–6.
- Taouli B, Vilgrain V, Dumont E, Daire JL, Fan B, Menu Y. Evaluation of liver diffusion isotropy and characterization of focal hepatic lesions with two single-shot echo-planar MR imaging sequences: prospective study in 66 patients. *Radiology.* 2003;226:71–8.
- Sinha S, Lucas-Quesada FA, Sinha U, DeBruhl N, Bassett LW. In vivo diffusion-weighted MRI of the breast: potential for lesion characterization. *J Magn Reson Imaging.* 2002;15:693–704.
- King AD, Ahuja AT, Yeung DW, Fong DKY, Lee YYP, Lei KIK, et al. Malignant cervical lymphadenopathy: diagnostic accuracy of diffusion weighted MR imaging. *Radiology.* 2007;245:806–13.
- Curvo-Semedo L, Lambregts DM, Maas M, Beets GL, Caseiro-Alves F, Beets-Tan RG. Diffusion-weighted MRI in rectal cancer: apparent diffusion coefficient as a potential noninvasive marker of tumor aggressiveness. *J Magn Reson Imaging.* 2012;35:1365–71.
- Kobayashi S, Koga F, Yoshita S, Masuda H, Ishii C, Tanaka H, et al. Diagnostic performance of diffusion-weighted magnetic resonance imaging in bladder cancer: potential utility of apparent diffusion coefficient values as a biomarker to predict clinical aggressiveness. *Eur Radiol.* 2011;21:2178–86.
- McVeigh PZ, Syed AM, Milosevic M, Fyles A, Haider MA. Diffusionweighted MRI in cervical cancer. *Eur Radiol.* 2008;18:1058–64.
- Cao K, Gao M, Sun YS, Li Y-L, Sun Y, Gao Y-N, et al. Apparent diffusion coefficient of diffusion weighted MRI in endometrial carcinoma—relationship with local invasiveness. *Eur J Radiol.* 2012;81:1926–30.
- Zbaren P, Weidner S, Thoeny HC. Laryngeal and hypopharyngeal carcinomas after (chemo)radiotherapy: a diagnostic dilemma. *Curr Opin Otolaryngol Head Neck Surg.* 2008;16:147–53.
- Dzik-Jurasz A, Domenig C, George M, Wolber J, Padhani A, Brown G, et al. Diffusion MRI for prediction of response of rectal cancer to chemoradiation. *Lancet.* 2002;360:307–8.

22. DeVries AF, Kremser C, Hein PA, Griebel J, Krezcy A, Öfner D, et al. Tumor microcirculation and diffusion predict therapy outcome for primary rectal carcinoma. *Int J Radiat Oncol Biol Phys*. 2003;56:958–65.
23. Kurosawa J, Tawada K, Mikata R, Ishihara T, Tsuyuguchi T, Saito M, et al. Prognostic relevance of apparent diffusion coefficient obtained by diffusion-weighted MRI in pancreatic cancer. *J Magn Reson Imaging*. 2015;42(6):1532–7.
24. Gahr N, Darge K, Hahn G, Kreher BW, von Buiren M, Uhl M. Diffusion-weighted MRI for differentiation of neuroblastoma and ganglioneuroblastoma/ganglioneuroma. *Eur J Radiol*. 2011;79(3):443–6.
25. Mahadevan D, Von Hoff DD. Tumor-stroma interactions in pancreatic ductal adenocarcinoma. *Mol Cancer Ther*. 2007;6:1186–97.
26. Koong AC, Mehta VK, Le QT, Fisher GA, Terris DJ, Brown JM, et al. Pancreatic tumors show high levels of hypoxia. *Int J Radiat Oncol Biol Phys*. 2000;48:919–22.
27. Semenza GL. HIF-1: mediator of physiological and pathophysiological responses to hypoxia. *J Appl Physiol*. 2000;88:1474–80.
28. Spivak-Kroizman TR, Hostetter G, Posner R, Aziz M, Hu C, Demeure MJ, et al. Hypoxia triggers hedgehog-mediated tumor-stromal interactions in pancreatic cancer. *Cancer Res*. 2013;73(11):3235–47.
29. Lewis S, Besa C, Wagner M, Jhaveri K, Kihira S, Zhu H, et al. Prediction of the histopathologic findings of intrahepatic cholangiocarcinoma: qualitative and quantitative assessment of diffusion-weighted imaging. *Eur Radiol*. 2018;28:2047–57.
30. Gültekin MA, Türk HM, Beşiroğlu M, Toprak H, Yurtsever I, Yilmaz TF, et al. Relationship between KRAS mutation and diffusion weighted imaging in colorectal liver metastases. Preliminary study. *Eur J Radiol*. 2020;125:108895.
31. Bruix J, Sherman M. Management of hepatocellular carcinoma. *Hepatology*. 2005;42:1208–36.
32. Huppertz A, Haraida S, Kraus A, Zech CJ, Scheidler J, Breuer J, et al. Enhancement of focal liver lesions at gadoteric acid-enhanced MR imaging: correlation with histopathologic findings and spiral CT-initial observations. *Radiology*. 2005;234:468–78.
33. Bolondi L, Gaiani S, Celli N, Golfieri R, Grigioni WF, Leoni S, et al. Characterization of small nodules in cirrhosis by assessment of vascularity: the problem of hypovascular hepatocellular carcinoma. *Hepatology*. 2005;42:27–34.
34. Weichert W, Röske A, Gekeler V, Beckers T, Ebert MPA, Pross M, et al. Association of patterns of class I histone deacetylase expression with patient prognosis in gastric cancer: a retrospective analysis. *Lancet Oncol*. 2008;9:139–48.
35. Romero Otero J, Garcia Gomez B, Campos Juanatey F, Touijer KA. Prostate cancer biomarkers: an update. *Urol Oncol*. 2014;32:252–60.
36. Lambregts DM, Vandecaveye V, Barbaro B, Bakers FCH, Lambrecht M, Maas M, et al. Diffusion-weighted MRI for selection of complete responders after chemoradiation for locally advanced rectal cancer: a multicenter study. *Ann Surg Oncol*. 2011;18:2224–31.
37. Intven M, Reerink O, Philipens ME. Diffusion-weighted MRI in locally advanced rectal cancer: pathological response prediction after neo-adjuvant radiochemotherapy. *Strahlenther Onkol*. 2013;189:117–22.
38. Fujimura M, Sakamoto S, Sekita N, Takeuchi N, Nishikawa R, Suzuki H, et al. Apparent diffusion coefficient value for estimating clinicohistological factors in bladder cancer including infiltration style and lymphatic invasion. *Springerplus*. 2016;5:848.
39. Shin HJ, Kim HH, Shin KC, Sung YS, Cha JH, Lee JW, et al. Prediction of low-risk breast cancer using perfusion parameters and apparent diffusion coefficient. *Magn Reson Imaging*. 2016;34:67–74.
40. He J, Shi H, Zhou Z, Chen J, Guan W, Wang H, et al. Correlation between apparent diffusion coefficients and HER2 status in gastric cancers: pilot study. *BMC Cancer*. 2015;15:749.
41. De Cobelli F, Ravelli S, Esposito A, Giganti F, Gallina A, Montorsi F, et al. Apparent diffusion coefficient value and ratio as noninvasive potential biomarkers to predict prostate cancer grading: comparison with prostate biopsy and radical prostatectomy specimen. *Am J Roentgenol*. 2015;204:550–7.
42. Fouladi DF, Zarghampour M, Pandey P, Pandey A, Varzaneh FN, Ghasabeh MA, et al. Baseline 3D-ADC outperforms 2D-ADC in predicting response to treatment in patients with colorectal liver metastases. *Eur Radiol*. 2020;30(1):291–300.
43. Ma T, Yang S, Jing H, Cong L, Cao Z, Liu Z, et al. Apparent diffusion coefficients in prostate cancer: correlation with molecular markers Ki-67, HIF-1 α and VEGF. *NMR Biomed*. 2018;31(3):e3884.
44. Shimomura M, Hinoi T, Kuroda S, Adachi T, Kawaguchi Y, Sasada T, et al. Overexpression of hypoxia inducible factor-1 alpha is an independent risk factor for recurrence after curative resection of colorectal liver metastases. *Ann Surg Oncol*. 2013;20:527–536.
45. Vaupel P, Harrison L. Tumor hypoxia: causative factors, compensatory mechanisms and cellular response. *Oncologist*. 2004;9:4–9.

How to cite this article: Yoshikawa M, Morine Y, Yamada S, et al. Prognostic prediction of resectable colorectal liver metastasis using the apparent diffusion coefficient from diffusion-weighted magnetic resonance imaging. *Ann Gastroenterol. Surg*. 2021;5:252–258. <https://doi.org/10.1002/ags3.12404>